Invited Paper

A new model for myosin dimeric motors incorporating Brownian ratchet and powerstroke mechanisms

Brian Geislinger and Ryoichi Kawai

Department of Physics, University of Alabama at Birmingham, Birmingham, AL 35294

ABSTRACT

A new dimer model is introduced to describe the behavior of dimeric processive motor proteins in general. A single motor domain is modeled using our previous work on hybrid motors that exhibit elements of both a powerstroke and a Brownian motor mechanism. The different behavior observed in Myosins V and VI can be explained by varying the physical parameters describing the coupling between the two motor domains. The dynamics of the resulting stepping mechanics under loaded and unloaded conditions are examined. The results from this dimer model are compared with experimental data for two-headed processive motors.

Keywords: Molecular motors, Brownian motors, power stroke, myosin V, myosin VI

1. INTRODUCTION

The myosin superfamily play key roles in a variety of intracellular transport processes. Although each member of the family exhibits quite different properties and functionalities, all of them share a similar mechanism for converting chemical energy into mechanical motion. In particular, they contain nearly identical motor domains, some have a single domain and others have two of them. The individual motor domains of these motor proteins cyclically bind and unbind from actin filament tracks by converting the chemical energy stored in ATP molecules into directed motion. As the motor progresses through ATP hydrolysis, the protein enters one of several different conformational states based on the current state of the nucleotide bound to the motor domain.[1–6] These conformational changes generate small changes in the neck region of myosin that result in the rotation of the tail end of the motor. These rotational motion is believed to be a driving force of the motor (power stroke model). On the other hand, the motors are subject to large thermal fluctuations due to collision with surrounding molecules. Some experimental data suggest that the motor proteins utilize the thermal fluctuations instead of fighting against them (Brownian motor model.) Recently, we developed a model for single headed motors which naturally unifies the power stroke and the Brownian motor models in a single picture.[7] In this proceedings, we extend our model to dimeric molecular motors.

Myosin V and Myosin VI are actin-based dimeric molecular motors. These particular classes of motor proteins are known for moving processively along an actin filament in that they both undergo numerous steps before completely dissociating from the actin filament. Non-processive motors, such as Myosin II, produce force generating cycles at comparatively long intervals, spending most of its time detached from the actin filaments. Muscle fibers only produce continuous forces through large numbers of Myosin II bundled together working in concert. On the other hand, Myosin V and other processive motor proteins produce motion as a single motor protein, not necessarily requiring the aid of other motors.[8,9] Instead, dimeric motor proteins coordinate the movement of their two motor domains in order to achieve processivity. Through some means of communication, the two motor domains alternate their attachment cycles so that at least one motor domain is attached to the filament at all times. Recent experiments suggest that force dependent chemical kinetics may act as the coordinating factor between the heads.[10–12] When the two motor domains are both in a strongly bound state to the filament, the leading motor creates a strained state between the two heads.[13] These experiments have shown that the forces in this strained state work with the chemical kinetics to favor a hand-over-hand mechanisms of motion along actin.

While these force dependent kinetics may provide a means of communication between the motor domains in a dimeric protein, the mechanism transporting individual motor domains from one binding site to the next

Further author information, send correspondence to Ryoichi Kawai (E-mail: kawai@uab.edu)

Noise and Fluctuations in Biological, Biophysical, and Biomedical Systems, edited by Sergey M. Bezrukov,
Proc. of SPIE Vol. 6602, 660206, (2007) · 0277-786X/07/$18 · doi: 10.1117/12.724693

remains unclear.[14,15] Many recent experiments have shown strong evidence of a hand-over-hand model of processive motion.[16–20] In this model, a strongly bound leading motor domain anchors the motor protein to the filament and swings the trailing motor domain forward $36\,nm$ into position for its next binding cycle. However, recent evidence showing the working stroke of a single Myosin V motor domain is only $25\,nm$[15] suggests that this transport mechanism may be more complicated. Subsequent experiments have resolved the full $36\,nm$ step length of Myosin V into $24\,nm$ and $12\,nm$ substeps.[21] It has been suggested that the latter substeps may be driven by thermal diffusion.

Myosin VI is another dimeric motor protein which moves along an actin filament in the opposite direction that Myosin V does.[22,23] Although the mechanism controlling the directionality of motor proteins has been a matter for debate, evidence suggests that Myosin VI moves in the negative direction by swinging its lever-arm in the opposite direction as Myosin V and other plus-end directed motor proteins.[22,24] Like myosin V, myosin VI processively travels with a step length of $36\,nm$, yet it has a much shorter neck length than Myosin V.[25–27] A single motor domain of Myosin VI produces a working stroke of only $18\,nm$.[28] Recent experiments suggest that the proximal region of the Myosin VI tail is flexible, unlike the rigid structure of Myosin V, allowing the two motor domains a longer reach than would otherwise be expected.[18,25,29,30] It is suggested that the diffusive process plays a much greater role in stretching the flexible regions than the power stroke.

There are other experimental data which support the Brownian motor mechanism. According to the powerstroke model, the size of the step that a protein makes should be directly proportional to the neck length of the protein. While some experiments on motor proteins with artificially shortened or lengthened neck domains have supported this claim,[31–37] the shorter neck length of Myosin VI is inconsistent with this theory. Others researchers have also observed similar inconsistency in motor proteins with artificially constructed neck regions.[28,38–43] Furthermore, a power stroke should produce a single step forward for every ATP molecule that a motor protein consumes. However recent advancements in single molecule experiments have observed that a single motor domain fragment is capable not only of taking multiple steps forward during the consumption of a single ATP but also occasionally taking backward steps.[25] These observations are indicative of a diffusive process involved as a single motor protein makes its way forward to its next binding site. As a result of these observations, many researchers have claimed that a Brownian ratchet mechanism may be involved in rectifying thermal fluctuations from the motor's environment into directed motion along the filament. On the other hand, the efficiency and loaded capacity of Brownian motors are too small to explain experimentally observed behavior.[9] It has been postulated that a combination of deterministic power stroke motion with some diffusive steps might be a probable explanation for the behavior of motor proteins.[14,15]

In the present work, we will present a dimer model to explain the qualitative behavior of processive motor proteins such as Myosins V and VI with two coupled motor domains. The model for a single motor domain has been detailed in our previous paper.[7] Using the full three chemical state expression of the monomer, we can take into account the key conformational states that have been experimental observed[1–3,5] and utilize both a powerstroke and Brownian motor mechanism during a single hydrolysis cycle as discussed earlier. In the following section, the mechanism for communication between the two motor domains will be explained. The resulting behavior of a dimer designed specifically for Myosins V and VI will be studied.

2. THE DIMER MODEL

Based on the assumption that large portions of the myosin motor protein are conserved in terms of structure and function from one type of myosin to another, the majority of the work presented in our previous paper[7] will be applied here as well. The individual motor domains of a dimeric processive motor protein will be represented by a three-state hybrid motor (see Fig. 1) designed to take advantage of both a Brownian motor mechanism as well as a powerstroke during every ATP hydrolysis cycle. The degree to which either mechanism will dominate depends on the physical parameters governing a given motors protein.

The three potentials that we choose corresponding to different states of the bound ATP nucleotides are given in general by

$$V_i(x,\theta) = \frac{K}{2}(\theta - \theta_i)^2 + U_i \cos\left[2\pi(x - \ell\theta)\right], \quad i \in (1,2,3) \tag{1}$$

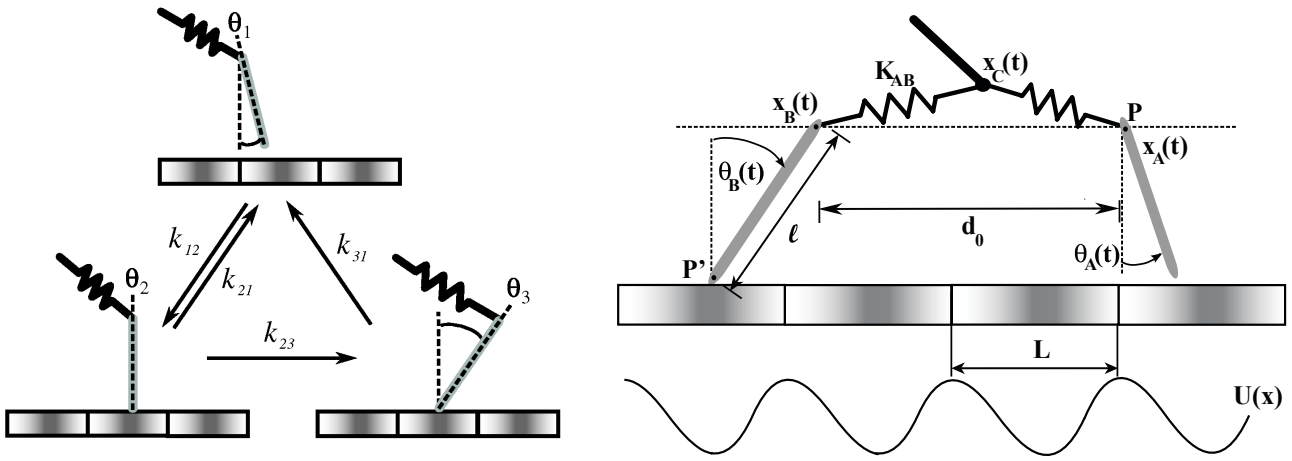

Figure 1. *Left*: One cycle of a three-state model for individual motor domains.[7] *Right*: A model for processive dimeric motor proteins. Two motor proteins individually driven by rotation-translation coupling interact through a loose spring. Each motor moves independently until the distance between the two stretches beyond an equilibrium length. The intramolecular strain caused by the two motors pulling on one another cause measurable changes in the ATP kinetics. These strain dependent rate changes provide a means for communication and coordination between the two motor domains.

where x and θ are respectively the position and orientation of an individual motor domain as shown in Fig. 1. The i-th state has a unique stable angle θ_i and potential strength U_i defining the interaction between the motor domain and the filament. For simplicity, we assume the periodicity of the filament potential $L = 1$. The rotation-translation coupling is generated by the $\cos[2\pi(x - \ell\theta)]$ term. As seen in Fig. 1, a single motor of length ℓ pivoting about a point P through and angle θ will result in the motor shifting forward a distance of approximately $\ell\Delta\theta$, which serves as a measure of the magnitude of the conformational change in the motor protein. A conformational change of $\ell\Delta\theta < L$ designates a motor relying on biasing thermal fluctuations; a powerstroke mechanism dominates for $\ell\Delta\theta > L$. The unbound state will be represented by U_1=0. The weakly bound and strongly bound states will have a strength of interaction $U_2 \ll U_3$. The conformational changes between the unbound and weakly bound state will be assigned a value $\ell\Delta\theta_{12} < 0.5$. The conformational change associated with the powerstroke as the motor domain enters the strongly bound state will be given by $\ell\Delta\theta_{23} \geq 1.0$. The rate of switching between the three states are given by k_{12}, k_{21}, k_{23}, and k_{31}. (See Fig. 1.) The rate limiting step of ATP hydrolysis in processive motor proteins is the release of ADP. As binding of new ATP molecules is typically considered diffusion limited, this rate limiting step corresponds to k_{31} in the above reaction scheme. Switching between these potentials periodically according to these rate constants give an inherent time dependency to $V(x, \theta)$. With the model for a single motor domain established, the nature of the coordination between the two motor domains in a dimeric motor protein must be addressed.

Recent observations that the intramolecular forces generated between the two motor domains of Myosin V can affect the chemical kinetics of ATP hydrolysis provide the basis for the current model of dimeric interaction. The rate limiting step of ATP hydrolysis, the release of ADP from the motor domain, has been observed to change significantly under load.[10,11] These experiments observed a decrease in the rate of ADP release when a backward load of approximately $2\,pN$ is applied to a single motor protein fragment. The assumption is that this backward force corresponds to the intramolecular strain a leading motor domain might feel from its trailing neighbor when both are in a strongly bound state. The leading motor would therefore be discouraged from releasing ADP and detaching from the filament while the other motor remains trailing behind it. Purcell, *et al.*[10] additionally observed a corresponding increase in that same rate when a similar forward force is applied to the motor fragment. This observation leads them to the conclusion that the forward strain that the trailing motor feels would encourage its release while the leading motor serves to anchor the motor protein.

Taking these observations into account, we design a switching method to coordinate the movements of the two motor domains. As the forward head reaches out and enters the strongly bound state the strain between

the two heads increases. The altered chemical kinetics resulting from this strain can be realized by the following simple expression governing the rate of entering and leaving the strongly bound state V_3

$$k'_{31} = k_{31}\sigma(|x_A - x_B|) \tag{2a}$$

$$\sigma(|x_A - x_B|) = 1 + \tanh\left(\frac{|x_A - x_B| - d_0}{\Delta d}\right), \tag{2b}$$

where $|x_A - x_B|$ represents the separation between motor domains A and B, d_0 is the critical separation between the two motor domains, and Δd is a measure of the sharpness of the interaction. Similar to the detailed model for Myosin V proposed in Ref. 44, this expression of the chemical kinetics allow the individual motors to move independent of one another for $|x_a - x_b| \ll d_0$ and triggers the strained kinetic mechanism for larger values of the separation between the heads.

The actual intramolecular forces on the individual motor domains can be approximated by simple springs attaching them to the tail of the motor protein x_C as shown in Fig. 1. Ensuring that the individual motor domains are reasonably free to move independent of one another by using a small value for the spring constant K_{AB}, we use an force interaction term of the form

$$F_{BA} = -K_{AB}(x_A - x_C - \frac{d_0}{2}) \tag{3a}$$

$$F_{AB} = -K_{AB}(x_B - x_C - \frac{d_0}{2}) \tag{3b}$$

$$F_C = -K_{AB}(2x_C - x_A - x_B - d_0) + F_{load} \tag{3c}$$

where F_{load} is an externally applied load on the tail of the motor protein.

Combining the above interaction with a carefully chosen set of parameters, it is possible to recreate the hand-over-hand behavior observed in processive motor proteins. Once ATP binds, releasing one of the motors, the process of searching for the next binding site begins. Assuming that the motor uses a Brownian ratchet mechanism to move to the next binding site, we choose V_1 and V_2 such that change in the stable angle $\Delta\theta$ is small (*i.e.*, within the Brownian ratchet regime for a single motor) and assume a shallow interaction with the filament (small U_i). Once the motor finds an appropriate binding site and the strain between the two heads increases, the transition to the third state V_3 becomes possible. This transition from V_2 to V_3 corresponds to the powerstroke of the motor and serves to anchor the protein while the other head releases and searches for its next binding site. Choosing the parameters for V_3 to reflect this behavior, $\ell\Delta\theta$ is large enough to deterministically reach adjacent potential wells and the binding strength U_3 is large. As the release of ADP is rate limiting, the rate of unbinding k_{31} is very slow compared with other stages of the reaction.

We can perform numerical analysis on the system described thus far by integrating the following set of overdamped Langevin equations of motion for each motor domain:

$$\dot{x}_A = -\frac{\partial V(x,\theta,t)}{\partial x} + \sqrt{2D}\ \xi_{xA} + F_{BA} \tag{4a}$$

$$\dot{\theta}_A = -\alpha\frac{\partial V(x,\theta,t)}{\partial \theta} + \sqrt{2\alpha D}\ \xi_{\theta A} \tag{4b}$$

$$\dot{x}_B = -\frac{\partial V(x,\theta,t)}{\partial x} + \sqrt{2D}\ \xi_{xB} + F_{AB} \tag{4c}$$

$$\dot{\theta}_B = -\alpha\frac{\partial V(x,\theta,t)}{\partial \theta} + \sqrt{2\alpha D}\ \xi_{\theta B} \tag{4d}$$

$$\dot{x}_C = F_C \tag{4e}$$

where the diffusion constant D and the dimensionless constant α are constants. The noise terms ξ_x and ξ_θ are defined independently for motor A and motor B. The time-dependent potential $V(x,\theta,t)$ alternately takes one of the potential values V_i according to the reaction rates k_{ij}. This coupled set of Langevin equations are integrated using the Heun method and the averages of motor positions are taken over a sufficient number of realizations.

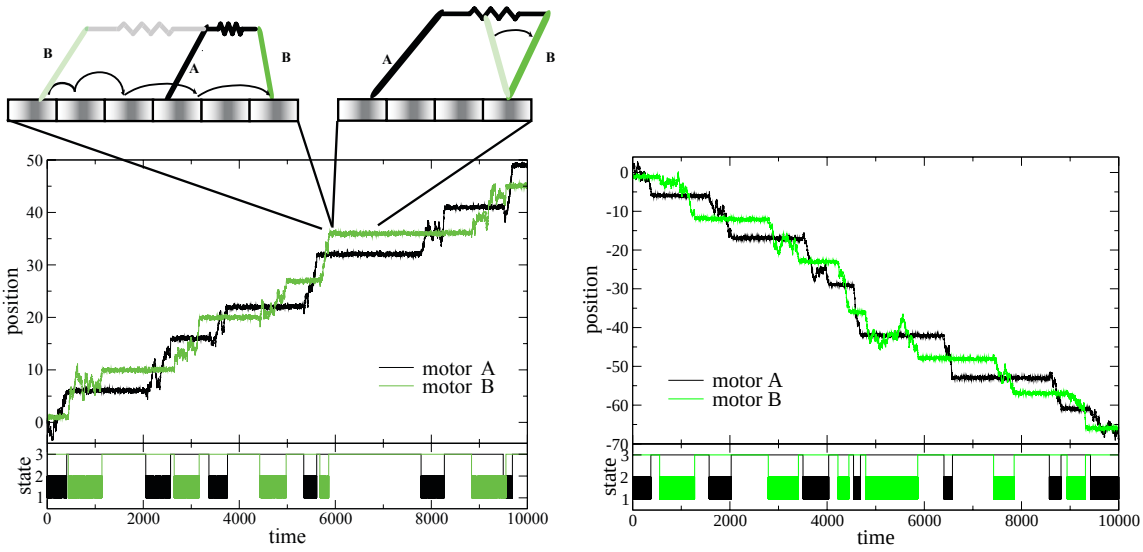

Figure 2. *Left*: Forward trajectory of a single dimer. The combination of the strain force and the strain dependent reaction rates easily allow for the two heads alternately moving past one another. Parameters: k_{12}=k_{21}=2.0, k_{23}=0.5, k_{31}=0.002, θ_1=-0.2, θ_2=0.0, θ_3=1.0; ℓ=1.0, K_{AB}=0.1, d_0=5.0, Δd=2.0. *Right*: Backward trajectory of a single dimer. Plotted here is the same dimer as the left panel with the direction of the lever arm motion reversed. Parameters: θ_1=0.2, θ_2=0.0, θ_3=-1.0.

While myosins V and VI exhibit very different properties, we can model both by adjusting the physical parameters set forth in the model above. Myosin VI is composed of a very short neck region compared with Myosin V, so we choose the motor length ℓ to be comparatively short. However, it is thought that the proximal tail region is highly flexible. While the degree of flexibility is not known, there is certainly evidence that the proximal tail has some degree of compliance.[18] To allow the motors to move in a fashion where the two motors are leashed together, free to move but still constrained, we define a small value for the spring constant K_{AB} connecting the two motors and a large value for d_0, the critical switching distance. Myosin V, on the other hand, has no evidence of compliance between the necks of the two motor domains. As a result we will use a large value for ℓ and K_{AB}, but a comparatively small value for d_0.

3. MYOSIN VI: A LEASHED DIMER

As seen in Fig. 2, the combination of the three state hybrid model and the strain coupling between the two motors in a dimer provides the desired hand-over-hand behavior. The two motors move in a coordinated fashion along the filament. The strongly bound state of one motor anchors the protein while the other switches between V_1 and V_2 to rectify thermal fluctuations and move forward to its next binding site. As the separation of the two heads approaches d_0, the searching motor anchors itself to the filament in V_3 and waits for the release of the trailing motor to repeat the process. The communication between the two motors gained through this strained state provides a low probability of both motors being in an unbound state at the same time. If both motors were to detach from the filament simultaneously, the assumption is that the processivity of the motor is broken. The present model allows for numerous ATP hydrolysis cycles to take place before the motor protein detaches permanently from the filament.

By reversing the sequence of stable angles through which the motors proceed during the ATP hydrolysis cycle, we obtain the behavior seen in Fig. 2. Mirroring the hand-over-hand behavior, this version of the motor protein walks in the opposite direction along the filament by merely changing this characteristic of the the motor domain as postulated by Wells, *et al.* and Tsiavaliaris, et al..[22,24]

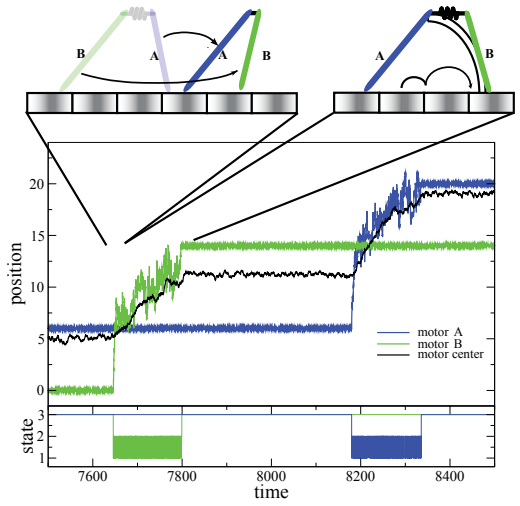

Figure 3. A detailed look at a Myosin V model. To examine the motion of Myosin V we plot the location of the motor center x_C, as well as the location of the binding end x_P for both motor A and motor B. Upon release of the trailing motor B. the strained leading motor A swings forward. Motor B then rectifies thermal fluctuations to increase its own strained state and move the remaining distance to its final binding site. The black outline behind motor B indicates how the strained state may appear given a compliant neck domain. Parameters: k_{12}=k_{21}=2.0, k_{23}=0.05, k_{31}=0.001; K_{AB}=1.0, d_0=5.6, Δd=2.0, ℓ=5.0.

In its present form, the model presented thus far is a reasonable model for a motor protein such as Myosin VI. Each motor domain essentially moves independent of the other until the separation between the heads reaches d_0. According to theories put forth by Rock, et al.,[30] it is possible that each motor domain of Myosin VI must move in such a manner. If indeed the protein contains long flexible neck domains allowing the motor to reach its full step length of 36 nm, then a diffusive process such as that provided by the Brownian motor mechanism is required to move the trailing motor forward. Here, the neck length of the motor is short, and as a result the powerstroke provides insufficient motion to explain the full step length of this motor. Most of the forward motion seen in the individual motor domain of this model occurs through the Brownian process between V_1 and V_2. On the other hand, the powerstroke of Myosin V makes a much larger contribution to the step distance of that motor variant. Additionally, the neck of Myosin V is not thought to be flexible as it is in Myosin VI. In order to more fully explain the motion of Myosin V a slightly modified model is required.

4. MYOSIN V: A TIGHTLY COUPLED DIMER

The full 36 nm step length of Myosin V can be achieved by extending the two 23 nm necks separated by an angle of $\sim 100°$.[45] While this stepping distance can be achieved by using this extended rigid structure to move in hand-over-hand manner, newer results suggest that the step of Myosin V is made in two or more substeps.[15,21] Modifying the dimer model to take the rigid nature of Myosin V into account, we set the spring K_{AB} connecting the two heads to be larger than in Myosin VI. Because of the tight coupling between the two heads, now the values of x_A and x_B will be nearly identical to x_C. As a result, the strain in the springs is not a plausible mechanism of communication between two domains. It is more likely that the strain associated with the neck rotation transmit the information. Therefore, instrad of Eq. (2) we adopt the following strain function:

$$\sigma(\theta_A, \theta_B) = 1 + \tanh\left(\frac{|\ell \sin\theta_A - \ell \sin\theta_B| - d_0}{\Delta d}\right). \tag{5}$$

Using this modified model, we see in Fig. 3 that the powerstroke for the leading motor occurs when the trailing motor releases from the filament. This powerstroke only produces a certain amount of forward displacement

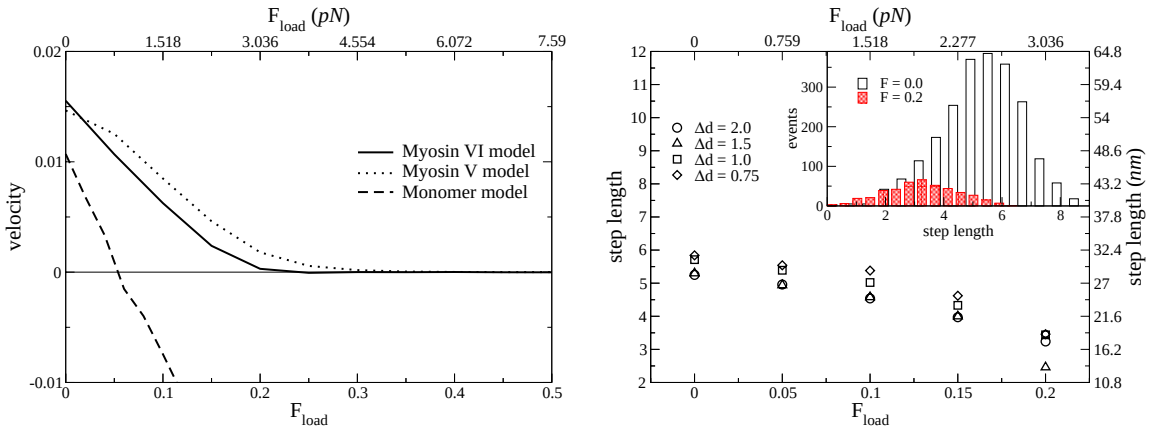

Figure 4. (a.) Force-velocity relationship of the dimer model compared with a single motor. (b.) Average step length for the Myosin V model. The distribution of step lengths for a myosin V molecule is examined under a variety of loaded conditions. Parameters: k_{12}=k_{21}=2.0, k_{23}=0.5, k_{31}=0.01; D=0.1, θ_1=-0.2, θ_2=0.0, θ_3=1.0.

forward, albeit a much larger displacement than that observed in Myosin VI. The remaining distance can be made up through a series of diffusive steps. Due to the long lever arm of Myosin V, the degree to which the motion is diffusive rather than deterministic resides in the magnitude of the angle change between V_1 and V_2, $\Delta\theta_{12}$. As determined in the previous chapter, thermal fluctuations can be rectified into directed motion in the case of $\ell\Delta\theta < 0.5$. For larger values, deterministic motion occurs as the long neck of Myosin V is able to step to adjacent potential wells even with small changes in the angle. The example trajectory in Fig. 3 shows that the forward motor can step out several more period length depending on the parameters chosen. A strained state is then created between the leading and trailing motor when the leading motor settles into a strongly bound state. The strain is primarily caused by the leading motor attempting to adopt the stable angle θ_3 while the trailing motor holds it back. This strained state is enhanced by the few additional steps made away from the trailing motor during the Brownian phase of motion. While there is no compliance in the neck of the motor in the present model, this strained state achieves similar results to the telemark-stance seen in electron micrograph images of Myosin V.[13] When the trailing motor releases, the strain in the leading motor is released quickly swinging forward the trailing motor a distance corresponding to the new stable angle of the leading motor, and the process is repeated.

5. LOADED DIMERS AND STEP DYNAMICS

By varying the constant F_{load} as stated in Eq. 3, we examine the force-velocity relationship of the dimer. The monomeric motor protein shown in Fig. 4(a) displays a linear relationship between its velocity and the magnitude of an applied load. Upon reaching its stall velocity at approximately $0.9\,pN$ (converting from normalized force units), the motor fails entirely sliding backwards under any additional load. On the other hand, the dimeric motor protein models exhibit a stall velocity of more than twice that of the monomer as seen in single headed versus double headed Myosin V experiments. Here, both the Myosin V and Myosin VI models stall at a force of approximately $3\,pN$. An additional feature shown in Fig. 4(a) is the monotonic decrease in the velocity as the dimers approach their stall force. Influenced by the anchoring function of the motor domains, the dimer complex apparently slows its hand-over-hand cycling as the applied load decreases the trailing motors ability to get into position for the next cycle. Once the stall velocity is reached the motor remains attached for long period of time, essentially stuck as the trailing motor is no longer capable of moving forward to trigger the chemical kinetic switch releasing the anchored motor. The anchored motor will only break free when the applied force is large enough to overcome the binding strength of the motor to the filament. On the other hand, a monomer or single headed motor operating under the same parameters stalls, but having no anchoring mechanism, it immediately breaks free of the filament.

To ascertain the detailed effect that an applied load has on the stepping mechanism of a dimeric motor protein governed by this model, we examine the step length of a motor under load. Here, we define the step length as the distance that the motor center x_C moves forward after each stepping event. Many single molecule experiments typically measure the displacement of an optically trapped glass microbead that would be attached to a point equivalent to x_C on the motor, therefore this definition of step length should have the most relevance to experiment. The distribution of step sizes of a Myosin V motor under loaded conditions is plotted in Fig. 4(b). In unloaded conditions, the distribution of steps is centered closely about the critical distance d_0 that triggers the chemical kinetics in Eq. 2. As the magnitude of the load is increased, the distance that the motor steps slowly decreases. The chemical kinetics remain unchanged and the ideal conditions for a trailing motor successfully stepping forward still occur when it reaches a distance d_0 in front of the anchored motor. While the shorter step length is not ideal, the searching motor spends enough time at a distance less than d_0 from the anchored motor that it still has a chance of entering a strongly bound state, albeit at a much slower rate. We can control the spatial window through which a motor must pass to activate the chemical switch in Eq. 2 by decreasing the value of Δd. By doing so, we shrink the tail of the spatial probability distribution defining the region where the searching motor finds it agreeable to enter a strongly bound state. Figure 4(b) shows that while smaller values of Δd increases the step length to some degree, the distribution of steps is still shifted towards zero for loads approaching stall force for the motor.

6. DISCUSSION

The proposition that the motion of dimeric motor proteins may be achieved through some combination of a powerstroke and a series of diffusive steps is a key element in the present model. Due to the insufficient length of the Myosin V powerstroke, it is thought that the additional distance is made up by another mechanism.[15] Myosin VI has an even shorter powerstroke and the majority of the distance covered in a single step must be realized through a diffusive mechanism. Despite their differences, both classes of myosin appear to have elements of a powerstroke mechanism as well as a Brownian motor mechanism. The model for a monomeric motor protein presented in the previous chapter provides a unified mechanism for generating both a powerstroke and thermally rectified motion. Using at least a three state cyclic system of chemical reactions incorporates both mechanisms by tuning the parameters governing each state.

While it may be difficult to verify that the method of coordination between the two heads used in the present model is an accurate biological representation, it is capable of replicating the hand-over-hand behavior observed experimentally. The model that we utilize coupling the two motors incorporates a strain mechanism for coordination between the two proteins based on the force dependent chemical kinetics that have been observed in recent experiments.[10–12] Using that mechanism the two otherwise independent motors are capable of coordinating their attachment cycles such that the chance that both motors are detached from the filament simultaneously becomes very small. Once anchored to the filament, the trailing motor then begins a search for its next binding site, using the Brownian ratchet mechanism provided by switching between V_1 and V_2. In the case of Myosin V where the value of ℓ is expected to be much larger than that of Myosin VI, a non-deterministic mechanism of motion can only be realized through very small changes in the neck angle between states 1 and 2. As single molecule experimental methods improve, smaller substeps have been resolved.[15,21] It is possible that even smaller, unresolved substeps that are a part of the ATP hydrolysis cycle may be responsible for Myosin V's ability to rectify thermal fluctuations into directed motion. Following the diffusive steps, the power stroke on entering state 3 induces enough strain between the two motors to signal trailing motor to release from the filament and begin its forward search. In addition, we were able to duplicate the motion seen in backwards moving motor proteins such as Myosin VI. One proposed mechanism for this behavior develops from the fact that the lever arm in Myosin VI swings in opposite direction of its Myosin V counterpart.[22] Simply by reversing the direction in the sequence of $\Delta\theta$ values as the reaction proceeds produces the desired behavior of a backward walking version of the Myosin V protein.

Watanabe *et al.*[46] reported that a single Myosin V motor domain produces a maximum force of $0.9\,pN$. A wild-type dimeric Myosin V produces an average maximum force of $2.4\,pN$, greater than twice the force of a single motor domain. Scaling back to SI units (1 unit $\approx$ 15 pN), the force-velocity relations plotted in Fig. 4(a) are in good agreement with these experimental results. The step size under loaded conditions plotted

in Fig. 4(b) also agree reasonably well with the experimental behavior observed by Altman, *et al.*[47] The authors of this experimental study claim that the step size remains unaffected as the load increases. However, the data published shows a slight decrease on the order of $\sim 10\,nm$ under a load of about $2\,pN$. Comparing these results to the drop in step size of roughly 2 potential periods L exhibited by this dimer model, for L equal to $5.4\,nm$ we have reasonably good agreement with experimental data.

In this same article Altman measures the dwelltime of the motor under loaded conditions. The stepping mechanics involved in moving a motor domain forward to its binding next site occur very quickly for most motor proteins. It is this fact that makes the stepping mechanics a difficult subject to study. These motor proteins spend the majority of their time bound to an actin filament waiting for the chemical reaction releasing it and allowing for the subsequent step. This slow chemical reaction is dominated by a Poisson process, and as such any measurement of a dwelling time will likewise be dominated by the same process. Loaded measurements of the dwelling time by Altman, *et al.* tell something about the force dependence of the chemical reactions governing the release of the motor protein, but a mechanical model such as the one presented here cannot faithfully reproduce these effects. As a result this Poisson process also causes some difficulty in attempting to compare the average velocity of our modeled motor proteins with their experimental counterparts. Proper modeling of this process in the long bound states is required to get an accurate scaling of the velocities of these models.

Looking also at the distribution of step sizes exhibited by the dimer, the chemical switch introduced to coordinate the hand-over-hand motion of the two motor domains also provides a degree of variation in the magnitude of the step size. This distribution of step sizes has been observed experimentally in numerous experimental studies[20,47,48] and has been a focus of other processive motor models.[49,50] In the limit as Δd approaches zero, the switch mechanism in Eq. 2 becomes a step function, only allowing searching motors to become strongly bound when it is a distance greater than d_0 forward of its partner motor. Tuning the parameter Δd should allow for fitting the step size distribution of the dimer model to any number of different experimentally observed step distributions.

The qualitative behavior of these processive, dimeric motor proteins can be replicated using this hybrid model that allows the individual motor domains to switch between alternate modes of transportation. While the mechanisms driving Myosins V and VI appear to be very different, many of the features can be replicated with this one model. Myosin V relies heavily, but not entirely, upon the powerstroke of the anchored motor, while Myosin VI favors the Brownian motor mechanism to transport its trailing head forward through its next step. Hopefully, by altering the physical parameters of this dimer model, a wide variety of motor proteins can be studied, each emphasizing different phases of the transport mechanism. And while the focus of this model was primarily on replicating the results seen in dimeric myosin-actin systems, it seems reasonable that this model could be extended to other families of processive motor proteins.

REFERENCES

1. I. Rayment, W. R. Rypniewski, K. Schmidt-Base, *et al.*, "Three-dimensional structure of myosin subfragment-1: A molecular motor," *Science* **261**, pp. 50–58, July 1993.
2. M. Whittaker, E. M. Wilson-Kubalek, J. E. Smith, *et al.*, "A 35-å movement of smooth muscle myosin on ADP release," *Nature* **378**, pp. 748–751, 1995.
3. J. D. Jontes, E. M. Wilson-Kubalek, and R. A. Milligan, "A 32° tail swing in brush border myosin I on ADP release," *Nature* **378**, pp. 751–753, 1995.
4. A. Houdusse, V. N. Kalabokis, D. Himmel, A. G. Szent-Gyorgyi, and C. Cohen, "Atomic structure of scallop myosin subfragment S1 complexed with MgADP: A novel conformation of the myosin head," *Cell* **97**, pp. 459–470, May 1999.
5. A. Houdusse, A. G. Szent-Gyorgyi, and C. Cohen, "Three conformational states of scallop myosin S1," *PNAS* **97**(21), pp. 11238–11243, 2000.
6. P. D. Coureux, H. L. Sweeney, and A. Houdusse, "Three myosin V structures delineate essential features of chemo-mechanical transduction," *EMBO J.* **23**(23), pp. 4527–4537, 2004.
7. B. Geislinger and R. Kawai, "Brownian molecular motors driven by rotation-translation coupling," *Phys. Rev. E* **74**, pp. 011912–10, July 2006.

8. S. Leibler and D. A. Huse, "Porters versus rowers: A unified stochastic model of motor proteins," *J. Cell Bio.* **121**, pp. 1357–1368, 1993.
9. J. Howard, *Mechanics of Motor Proteins and the Cytoskeleton*, Sinauer Associates, Inc., Sunderland, MA, 2001.
10. T. J. Purcell, H. L. Sweeney, and J. A. Spudich, "A force-dependent state controls the coordination of processive myosin V," *PNAS* **102**(39), pp. 13873–13878, 2005.
11. C. Veigel, S. Schmitz, F. Wang, and J. R. Sellers, "Load-dependent kinetics of myosin-V can explain its high processivity," *Nat. Cell Biol.* **7**, pp. 861–869, 2005.
12. A. E.-M. Clemen, M. Vilfan, J. Jaud, J. Zhang, M. Barmann, and M. Rief, "Force-Dependent Stepping Kinetics of Myosin-V," *Biophys. J.* **88**(6), pp. 4402–4410, 2005.
13. M. L. Walker, S. A. Burgess, J. R. Sellers, F. Wang, J. A. Hammer, J. Trinick, and P. J. Knight, "Two-headed binding of a processive myosin to F-actin," *Nature* **405**(6788), pp. 804–807, 2000.
14. M. A. Geeves, "Molecular motors: Stretching the lever-arm theory," *Nature* **415**, p. 129, 2002.
15. C. Veigel, F. Wang, M. L. Bartoo, J. R. Sellers, and J. E. Molloy, "The gated gait of the processive molecular motor, myosin V," *Nat. Cell Biol.* **4**, pp. 59–65, Jan. 2002.
16. J. N. Forkey, M. E. Quinlan, M. A. Shaw, J. E. T. Corrie, and Y. E. Goldman, "Three-dimensional structural dynamics of myosin V by single-molecule fluorescence polarization," *Nature* **422**, p. 399, 2003.
17. A. Yildiz, J. N. Forkey, S. A. McKinney, *et al.*, "Myosin V walks hand-over-hand: Single fluorophore imaging with 1.5-nm localization," *Science* **300**, pp. 2061–2065, 2003.
18. Z. Okten, L. S. Churchman, R. S. Rock, and J. A. Spudich, "Myosin VI walks hand-over-hand along actin," *Nat. Struc. Mol. Biol.* **11**(9), pp. 884–887, 2004.
19. K. Kinosita, M. Y. Ali, K. Adachi, K. Shiroguchi, and H. Itoh, "How two-foot molecular motors may walk," *Advances in Experimental Medicine and Biology* **565**, pp. 205–219, 2005.
20. D. M. Warshaw, G. G. Kennedy, S. S. Work, E. B. Krementsova, S. Beck, and K. M. Trybus, "Differential Labeling of Myosin V Heads with Quantum Dots Allows Direct Visualization of Hand-Over-Hand Processivity," *Biophys. J.* **88**(5), pp. L30–32, 2005.
21. S. Uemura, H. Higuchi, A. O. Olivares, E. M. De La Cruz, and S. Ishiwata, "Mechanochemical coupling of two substeps in a single myosin V motor," *Nat. Struc. Mol. Biol.* **11**(9), pp. 877–883, 2004.
22. A. L. Wells, A. W. Lin, L. Chen, D. Safer, S. M. Cain, T. Hasson, B. O. Carragher, R. A. Milligan, and H. L. Sweeney, "Myosin VI is an actin-based motor that moves backwards," *Nature* **401**, pp. 505–08, 1999.
23. K. Homma, M. Yoshimura, J. Saito, R. Ikebe, and M. Ikebe, "The core of the motor domain determines the direction of myosin movement," *Nature* **412**(6849), pp. 831–834, 2001.
24. G. Tsiavaliaris, S. Fujita-Becker, and D. J. Manstein, "Molecular engineering of a backwards-moving myosin motor," *Nature* **427**, p. 558, 2004.
25. R. S. Rock, S. E. Rice, A. L. Wells, T. J. Purcell, J. A. Spudich, and H. L. Sweeney, "Myosin VI is a processive motor with a large step size," *PNAS* **98**(24), pp. 13655–13659, 2001.
26. S. Nishikawa, K. Homma, Y. Komori, M. Iwaki, T. Wazawa, A. Hikikoshi Iwone, J. Saito, R. Ikebe, E. Katayama, T. Yanagida, and M. Ikebe, "Class vi myosin moves processively along actin filaments backward with large steps," *Biochem. Biophys. Res. Commun.* **290**, pp. 311–317, Jan. 2002.
27. M. Y. Ali, K. Homma, A. H. Iwane, *et al.*, "Unconstrained steps of myosin VI appear longest among known molecular motors," *Biophys. J.* **86**(6), pp. 3804–3810, 2004.
28. I. Lister, S. Schmitz, M. Walker, *et al.*, "A monomeric myosin VI with a large working stroke," *EMBO J.* **23**(8), pp. 1729–1738, 2004.
29. A. Yildiz, H. Park, D. Safer, Z. H. Yang, L. Q. Chen, P. R. Selvin, and H. L. Sweeney, "Myosin VI steps via a hand-over-hand mechanism with its lever arm undergoing fluctuations when attached to actin," *J. Biol. Chem.* **279**, pp. 37223–37226, Sept. 2004.
30. R. S. Rock, B. Ramamurthy, A. R. Dunn, S. Beccafico, B. R. Rami, C. Morris, B. J. Spink, C. Franzini-Armstrong, J. A. Spudich, and H. L. Sweeney, "A flexible domain is essential for the large step size and processivity of myosin VI," *Mol. Cell* **17**, pp. 603–609, Feb. 2005.
31. M. Anson, M. A. Geeves, S. E. Kurzawa, *et al.*, "Myosin motors with artificial lever arms," *EMBO J.* **15**(22), pp. 6069–6074, 1996.

32. T. Q. P. Uyeda, P. D. Abramson, and J. A. Spudich, "The neck region of the myosin motor domain acts as a lever arm to generate movement," *PNAS* **93**, pp. 4459–4464, 1996.
33. T. Sakamoto, F. Wang, S. Schmitz, *et al.*, "Neck length and processivity of myosin V," *J. Bio. Chem.* **278**(31), pp. 29201–29207, 2003.
34. T. J. Purcell, C. Morris, J. A. Spudich, *et al.*, "Role of the lever arm in the processive stepping of myosin V," *PNAS* **99**(22), pp. 14159–14164, 2002.
35. D. H. Schott, R. N. Collins, and A. Bretscher, "Secretory vesicle transport velocity in living cells depends on the myosin-V lever arm length," *J. Cell. Biol.* **156**(1), pp. 35–39, 2002.
36. C. Ruff, M. Furch, B. Brenner, *et al.*, "Single-molecule tracking of myosins with genetically engineered amplifier domains," *Nat. Struc. Biol.* **8**(3), pp. 226–229, 2001.
37. D. M. Warshaw, W. H. Guilford, Y. Freyzon, *et al.*, "The light chain binding domain of expressed smooth muscle heavy meromyosin acts as a mechanical lever," *J. Biol. Chem.* **275**, pp. 37167–37172, 2000.
38. A. Ishijima, H. Kojima, T. Funatsu, *et al.*, "Simultaneous observation of individual ATPase and mechanical events by a single myosin molecule during interaction with actin," *Cell* **92**, pp. 161–71, 1998.
39. S. Itakura, H. Yamakawa, Y. Y. Toyoshima, *et al.*, "Force-generating domain of myosin motor," *Biochem. Biophys. Res. Commun.* **196**(3), pp. 1504–1510, 1993.
40. K. M. Trybus, E. Krementsova, and Y. Freyzon, "Kinetic characterization of a monomeric unconventional myosin V construct," *J. Biol. Chem.* **274**(39), pp. 27448–27456, 1999.
41. C. Perreault-Micale, A. D. Shushan, and L. M. Coluccio, "Truncation of a mammalian myosin I results in loss of Ca2+-sensitive motility," *J. Biol. Chem.* **275**(28), pp. 21618–21623, 2000.
42. K. Homma, J. Saito, R. Ikebe, *et al.*, "Ca2+-dependent regulation of the motor activity of myosin V," *J. Biol. Chem.* **275**(44), pp. 34766–34771, 2000.
43. H. Tanaka, K. Homma, A. H. Iwane, *et al.*, "The motor domain determines the large step of myosin-V," *Nature* **415**, pp. 192–95, 2002.
44. G. H. Lan and S. X. Sun, "Dynamics of myosin-v processivity," *Biophys. J.* **88**(2), pp. 999–1008, 2005.
45. A. D. Mehta, R. S. Rock, M. Rief, J. A. Spudich, M. S. Mooseker, and R. E. Cheney, "Myosin-V is a processive actin-based motor," *Nature* **400**(6744), pp. 590–593, 1999.
46. T. M. Watanabe, H. Tanaka, A. H. Iwane, S. Maki-Yonekura, K. Homma, A. Inoue, R. Ikebe, T. Yanagida, and M. Ikebe, "A one-headed class V myosin molecule develops multiple large (≈ 32-nm) steps successively," *PNAS* **101**, pp. 9630–9635, 2004.
47. D. Altman, H. L. Sweeney, and J. A. Spudich, "The mechanism of myosin VI translocation an its load-induced anchoring," *Cell* **116**(5), pp. 737–749, 2004.
48. J. C. M. Gebhardt, A. E.-M. Clemen, J. Jaud, and M. Rief, "Myosin-V is a mechanical ratchet," *PNAS* **103**, pp. 8680–8685, 2006.
49. P. Xie, S. Dou, and P. Wang, "A hand-over-hand diffusing model for myosin-VI molecular motors," *Biophys. Chem.* **In Press, Corrected Proof**, pp. –, 2006.
50. G. H. Lan and S. X. Sun, "Dynamics of myosin-driven skeletal muscle contraction: I. steady-state force generation," *Biophys. J.* **88**(6), pp. 4107–4117, 2005.